Experimental and DFT Study of the [AuAr(AsPh$_3$)]-Catalyzed *cis/trans* Isomerization of [PdAr$_2$(AsPh$_3$)$_2$] (Ar = C$_6$F$_5$ or C$_6$Cl$_2$F$_3$): Alternative Mechanisms and its Switch upon Pt for Pd substitution

Pedro Villar,[b] Mónica H. Pérez-Temprano,[a] Juan A. Casares,*,[a] Rosana Álvarez,*,[b] and Pablo Espinet.*,[a]

[a] IU CINQUIMA/Química Inorgánica, Facultad de Ciencias, Universidad de Valladolid, 47071-Valladolid (Spain).

[b] Departamento de Química Orgánica, Facultade de Química, CINBIO and IIS Galicia Sur, Universidade de Vigo, E-36310, Vigo, (Spain)

ABSTRACT: The aryl transmetalation processes between *cis*-[PdRf$_2$(AsPh$_3$)$_2$] (Rf = C$_6$Cl$_2$F$_3$) and [AuPf(AsPh$_3$) (Pf = C$_6$F$_5$) has been studied experimentally and by DFT calculations. Aryl exchange with or without isomerization of the Pd geometry occur by ligand displacement of one AsPh$_3$ ligand by an AuAr(AsPh$_3$) molecule, which coordinates using the Au–Ar bond electron density, followed or not by a second switch to the next Ar group. The transition states are bridged Ar–Au(AsPh$_3$)–Ar' structures with fairly planar geometry. Alternatively, a direct switch of the Au(AsPh$_3$) fragment to either cis or trans Ar groups on Pd can be achieved from a square-pyramidal [(AsPh$_3$)Au-PdAr$_3$(AsPh$_3$)] intermediate or transition state. The later pathway is less favorable for the case studied (M = Pd), but it is preferred for the same chemical system with M = Pt. The study provides some clues on exchanges that can be relevant in organic syntheses catalyzed by bimetallic systems.

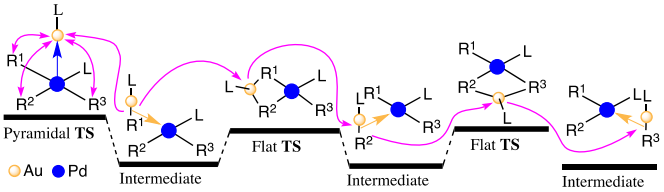

Introduction

In 1998 we reported that just 0.6 mol% of [AuRf(tht)] (Rf = C$_6$Cl$_2$F$_3$ = 3,5-dichloro-2,4,6-trifluorophenyl) catalyzed the isomerization of *trans*-[Pd(Rf)$_2$(tht)$_2$] (tht = tetrahydrothiophene) to the *cis* complex within minutes.[1] In the absence of gold, this isomerization takes hours. Although usually forgotten in the reviews, this seems to be the first reported example of a gold(I)-catalyzed reaction, and the first mechanistic study as well. Experiments carried out mixing palladium and gold complexes bearing C$_6$Cl$_2$F$_3$ (Rf) and C$_6$F$_5$ (Pf) groups revealed that the Au^{I}-catalyzed isomerization takes place with Au^{I}/Pd^{II} aryl exchange. A mechanism through species involving Au-Pd interactions was proposed (Scheme 1) based on reported X-ray structures of Pt^{II}/Au^{I} and Pt^{II}/Ag^{I} bimetallic complexes.[2] At that time there were no similar structural studies of Au-Pd complexes.

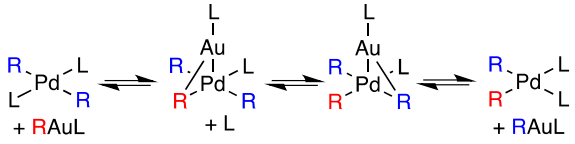

Scheme 1. Au catalyzed isomerization: Mechanistic proposal in 1998.

Quantitative kinetic studies of the fast isomerization for L = tht, and theoretical calculations were not accessible to us at that time. In the meantime the recent popularization in organic synthesis of bimetallic catalysis,[3] where two transition metals (including the Cu group for short in this definition) cooperate, has enhanced the mechanistic relevance of that study: the aryl exchanges observed can account for the transmetalations occurring in some bimetallic catalyses.

Since that seminal study, a number of complexes have been reported for systems with M = Pd^{II}, Pt^{II} and M' = Au^{I}, Ag^{I}, Cu^{I},[4-12] containing Pd-Au interactions that resemble, more or less closely, the M-M' interactions proposed in reference 1 for the intermediates or transition states shown in Scheme 1. It might look far-fetched to think that the exchange (and isomerization) model based on formation of M–M' interactions at short distances could be found for less similar metal centers, but the fact is that in our theoretical mechanistic studies on the ZnMe$_2$-catalyzed *cis/trans* isomerization of [PdMeAr(PR$_3$)$_2$] complexes (Ar = C$_6$Cl$_2$F$_3$ and C$_6$F$_5$) we found Zn^{II} playing a structural role quite similar to that of Au^{I} in Scheme 1.[13,14] Thus, in all the cases discussed above (M = Pd^{II}, Pt^{II}; M' = Au^{I}, Ag^{I}, Cu^{I}, Zn^{II}), experimental or theoretical data reveal structures with short M-M' distances (in the order of the sum of covalent radii distances) and three-center two-electron (3c2e) electron-deficient M–C–M' bridges. The M–C–M' angle (whether in intermediates or in transition states (TS) can vary from close to 90° to much smaller.

In the last years, many examples of coupling reactions involving R-for-X Pd/Au transmetalations have been reported, in which organogold complexes participate as stoichiometric reagents,[8-21] or are used as co-catalyst.[22-28] The transmetalation reaction has been studied in some cases by computational methods, but experimental quantitative data are scarce.[29-33] In 2012 we reported a kinetic and computational study on the Rf/Cl exchange (transmetalation) between [PdRf$_2$L$_2$] and [AuClL] (L = AsPh$_3$).[29] In that work we proposed that [AuClL], acting as "incoming ligand", substituted one L ligand at the palladium complex; at that step the transition state displayed a Pd–Au interaction. This pathway was soon backed by the proposal of Hashmi for the vinyl/X transmetalation between [PdRXL$_2$] and [Au(vinyl)L] (L =

PMe_3), which additionally demonstrated a small increase in $\Delta G^{‡}$ on moving from X = I to X = Cl.[30] A computational study of the transmetalation of alkynylgold complexes to palladium was reported more recently by Larsen and Nielsen, in a work concerning the Au/Cu/Pd co-catalyzed Sonogashira reaction,[32] Other computational studies on Au/Pd transmetalations and Pd complexes have been recently published by Yates.[31,33] Note that none of these studies deals with the simultaneous exchange of two organic groups between gold and palladium (*i.e,* R-for-R' Pd/Au exchange). This makes a difference between the transition states proposed in those studies, where the TS contains one non-deficient Au–X–Pd bridge in addition to one electron-deficient Au–C–Pd bridge (Figure 1a), and the TS required for the mechanism proposed in our first report,[1] which should contain two electron-deficient Au–C–Pd bridges (Figure 1b).

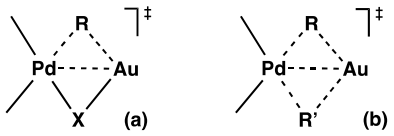

Figure 1. R/X or R/R' transmetalation transition states.

As an additional variation concerning transmetalation mechanisms, in our recent study on RhR/AuR' transmetalation, we have found a dramatic mechanistic switch. This transmetalation does not follow the classical and now generally assumed double-bridge mechanism commented above. On the contrary, the exchange is the consequence of a reversible oxidative addition/reductive elimination process, where the LAu–R' bond oxidatively adds to Rh^{I}. After isomerization of the resulting octahedral complex, reductive elimination of LAu–R completes the exchange process.[34] Obviously, the oxidation of Rh^{I} is much easier than the oxidation of Pd^{II}. This explains the accessibility to this new mechanism with Rh^{I} and, so far, not with Pd^{II}.

In summary, although mechanistic studies on bimetallic systems combining theoretical and experimental data are still scarce, many very recent Pd or Pt studies have added plausibility to our 1998 proposal. Moreover, he relevance of that early study, investigating Ar transmetalation between different metals and their relationship with isomerization, has gained interest in present times, when bimetallic processes are receiving much attention, and when it is unquestionable that isomerization is essential for many TM catalysis, even only rarely are this step specified in the simplified catalytic cycles.[35] Here we are revisiting that study using experimental, kinetic, and theoretical methodologies not available to us at that time. Furthermore, we undertake the study of the kinetics of the PdRf/AuPf exchange, which has a complexity that we had to spare in our initial study focusing on the simplified PdRf/AuRf exchange. The new study allows us to discriminate the kinetics of exchanges with or without isomerization at the palladium complex. The DFT calculations, carried out on the real molecules, provide information on the whole mechanistic profile, in part experimentally non-accessible, and matches very well the kinetic experimental observations.

Results and Discussion. In order to get experimental information from the kinetic studies, we had first to find an L ligand producing the isomerization (and the other competitive exchanges) at rates that could be accurately measured by ^{19}F NMR at a comfortable temperature. PPh_3 was too slow and tht was too fast, supporting that at some point of the mechanism the ancillary ligand has to be released. $AsPh_3$ provided measurable rates at 323 K. Thus, we have carried out kinetic studies on the system formed by *cis*-[$PdRf_2(AsPh_3)_2$] (**1a**), its isomer *trans*-[$PdRf_2(AsPh_3)_2$] (**2a**), and [AuPf($AsPh_3$) (**3a**). The use of different aryl groups in Pd and Au allows us to identify and measure independently aryl exchanges with or without isomerization. Pf and Rf complexes are thermodynamically very similar, and their combined use facilitates monitoring by ^{19}F NMR the exchanges, in a way quite similar to isotopic labeling.[36,37] Finally, the use of the same ligand for Pd and Au avoids a bewildering panorama having to account for different ligand dissociation energies and formation of new complexes due to L/L' exchanges. The monodentate L ligand is not significant for the essence of the aryl exchange mechanisms, although it can be kinetically decisive for the success of the catalysis.[27]

The isomerization reactions with $AsPh_3$ as ligand are very slow compared to those previously studied with tht.[1] In the absence of any gold catalyst the spontaneous isomerization of **1a** to **2a** is only 8% after 24 hours at 323 K.[38] Consequently non-catalyzed contribution when measuring the much faster gold-catalyzed reactions is negligible in the initial 1.5 hours. After 24 hours of catalyzed isomerization at 323, the system has reached equilibrium (a similar result is obtained when Pf is used on Pd and Au instead of Rf), with K_{iso} = [**2a**]/[**1a**] = 4.[39] The kinetics of the reaction is first order in [**3a**]. Experiments on the effect of added $AsPh_3$ show a strong retarding effect of the ligand at the beginning of the process, with $[AsPh_3]^{-1}$ kinetic order.[40] The observed initial rates fit well equation 1, which is a typical rate law for a two-step mechanism where the first step is the substitution of one $AsPh_3$ by the incoming reagent (complex **3a**), and the second (and rds one) leads to the final products. The activation energy of this reaction is 25.8 kcal/mol (see SI for kinetic details).

$$r_{iso} = \frac{a[\mathbf{1a}][\mathbf{3a}]}{b + c[\mathrm{AsPh_3}]} \qquad \text{(eq. 1)}$$

The mechanistic information extracted from these experiments with identical Ar groups on both metals does not reveal whether isomerization and aryl exchange are univocally connected or, on the contrary, there are aryl exchanges that do not lead to isomerization. This can be disclosed studying the process *cis*-[$PdRf_2(AsPh_3)_2$] (**1a**) + [AuPf($AsPh_3$)] (**3b**), with a different aryl group at each metal center. C*is*- and *trans*-diaryl palladium complexes containing the two groups, Pf and Rf, are formed. If all the cis and trans complexes are summed up (*cis* = **1a** + **1ab** + **1b**; *trans* = **2a** + **2ab** + **2b**) the neat cis/trans isomerization profile for this system is identical to that formed by **1a** + **3a**, whether with or without arsine excess in solution, confirming the thermodynamic *quasi*-equivalence of the Rf and Pf groups. Using this *"aryl labeling"* we can monitor and identify by ^{19}F NMR the aryl exchanges that bring about isomerization, and those that do not. The complexes involved are labeled in Scheme 2 where, for the sake of simplicity not all the operating reactions leading to each same product are represented. The experimental observations, immediately confirm the operation of AuPf/PdRf exchanges producing [AuRfL] and [$PdRfPfL_2$] complexes, which in turn become the subject of new exchanges. There will be also *"kinetically unproductive"* exchanges (*e.g.* AuRf/PdRf exchanges) that are unobservable unless they produce isomerization or a second substitution on Pd. The use of all the experimental information

available provides relevant clues on the several reaction pathways actually operating in the system.[36]

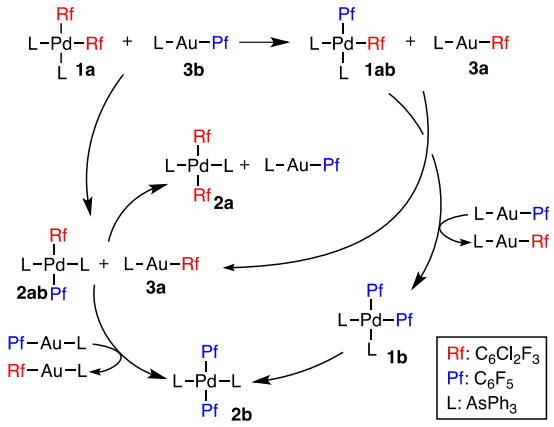

Scheme 2. Products observed in Figure 2, formed from **1a** and **3b** by scrambling of Rf and Pf between metals. All the arrows must be understood as reversible equilibria.

Figure 2 plots the evolution of the reaction **1a** + **3b**. In the initial 1.5 hours the main reaction products are *cis*-[Pd(Rf)(Pf)($AsPh_3$)$_2$] (**1ab**) and [AuRf($AsPh_3$)] (**3a**), supporting that the aryl exchange between gold and palladium with retention of the starting cis geometry at Pd is faster than the process coursing with cis/trans isomerization. At that moment (1.5 h), the **3b**/**3a** ratio has reached the statistical equilibrium distribution of aryl groups in the mixture. This ratio will not change in the subsequent time. Also, the concentration of **1ab** has reached equilibrium with **1a**, supporting again the thermodynamic similarity of Pf and Rf. Finally, a small amount of *cis*-[Pd($Pf)_2$($AsPh_3$)$_2$] (**1b**), requiring two exchanges, has been formed. After this initial period, the concentrations of the *cis* isomers **1a** and **1ab** decay at the same pace (**1ab** virtually disappears), producing the thermodynamically preferred trans isomers **2a** + **2ab**, and a small amount of the double-substitution product **2b**.

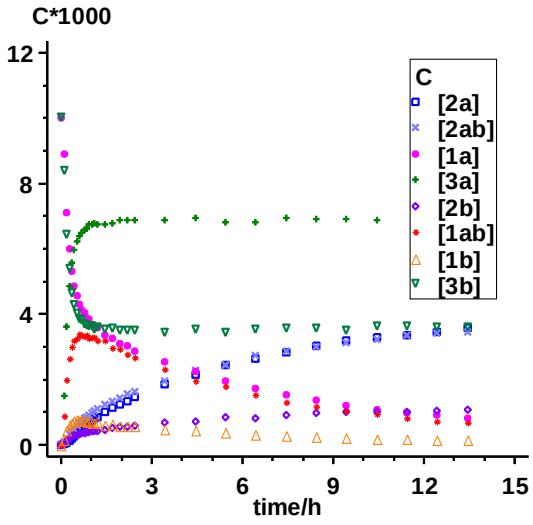

Figure 2. Concentration-time plots for the 1:1 reaction of cis-[Pd($C_6Cl_2F_3$)$_2$($AsPh_3$)$_2$] (**1a**) with [Au(C_6F_5)($AsPh_3$)] (**3b**) in $CDCl_3$ at 323 K. Starting conditions: [**1a**]$_0$ = 0.01 M; [**3b**]$_0$ = 0.01 M.

The kinetic behavior of the aryl exchange reaction was fit to a model that starts with the substitution of one $AsPh_3$ ligand in Pd by the incoming molecule of gold catalyst. This is followed either by the faster aryl exchange with retention of geometry at palladium, or by the slower one with isomerization (Figure 3). The respective experimental $\Delta G_{323}^{\ddagger}$ values obtained were 25.1 and 26.6 kcal×mol^{-1}, which fit very well the overall experimental observations.

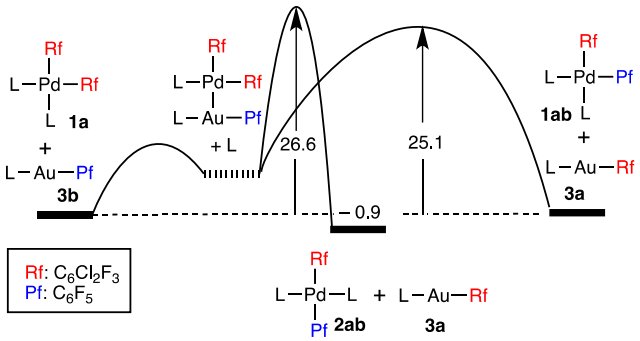

Figure 3. Simplified kinetic pathways proposed for transmetalation with or without isomerization. (See supplementary information for details). Values for activation energies by mathematical fitting are in kcal×mol^{-1}.

A DFT study[41] for a more complete description of the multistep reaction pathways has to consider the following cases: *i)* Pf/Rf exchange pathways with geometrical retention, or with *cis/trans* isomerization; and ii) successive gold migrations to contiguous aryls, or direct gold migration between mutually trans aryls. Figure 4 shows the calculated profile leading to *cis/trans* isomerization, which consists of incorporation of the gold complex to the *cis* Pd-complex through **TS1**, followed by one single gold *cis*-migration to a contiguous aryl (**I2**), and by [AuArL] decoordination via L coordination to Pd through **TS3** (black lines). This produces **3a** and a *trans* Pd complex (**2ab**) with one aryl exchanged.[42]

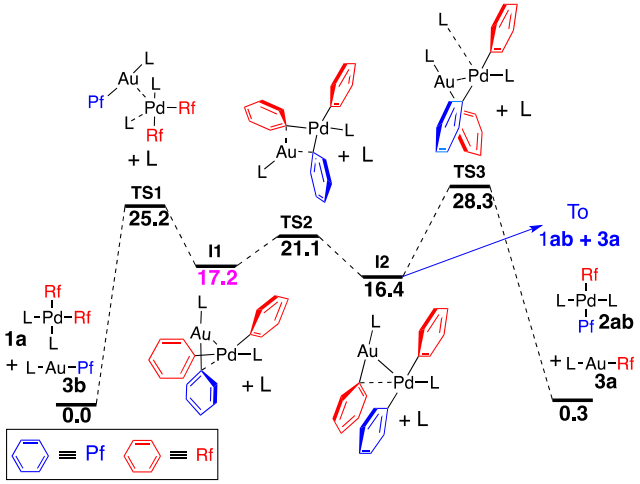

Figure 4. Calculated pathway for the aryl exchange between **1a** and **3b** to produce **2ab** and **3a**. This pathway changes the *cis/trans* geometry at the palladium complex.

The pathway leading to retention of the initial *cis* configuration is shown in Figure 5 in blue lines: from intermediate **I2** the AuL fragment can easily migrate to the adjacent fluoroaryl through **TS4** leading to **I3**, from which **3a**

is released upon $AsPh_3$ recoordination yielding **1ab**. Overall, the process requires two successive *cis*-migrations of AuL.

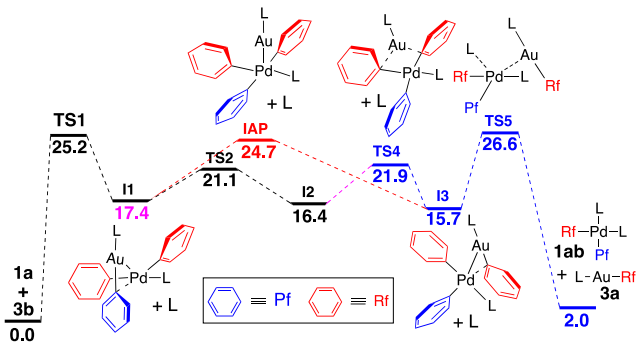

Figure 5. *Blue lines*: Calculated pathway of aryl exchange with retention of the *cis* geometry, giving **1ab.** *Red lines:* Calculated direct Au-*trans*-exchange (with geometrical retention) through species with AuL coordinated in apical position.

Reiteration of the two profiles just discussed, now involving in the reaction the new Au and Pd complexes formed in the first run, can give rise to all the species observed in the experiments (Figure 2) and shown in Scheme 2. The first step of all the exchange processes for the reaction **1a** + **3b** (whether forward or backward) is the substitution of one $AsPh_3$ by the incoming gold complex, producing intermediate **I1**; the last step is the release of the leaving gold complex upon arsine coordination, either from **I2** via **TS3** (Figure 4) or from **I3** via **TS5** (Figure 5). These steps are rate determining and the rest of changes occur with clearly lower activation energies within the range 21-22 kcal×mol^{-1}. The profile with retention of geometry is almost symmetrical (25.2 kcal×mol^{-1} for **TS1** and 26.6 kcal×mol^{-1} for **TS5**). However, **TS3** is rate determining for the process with *cis/trans* exchange, whether in the forward or in the backward reaction.

Our calculations predict a slower rate for the process with isomerization yielding **2ab** + **3a** (ΔG**TS3** = 28.3 kcal×mol^{-1}), than for the one with geometry retention yielding **1ab** + **3a** (ΔG**TS5** = 26.6 kcal×mol^{-1}). The reason is that in **TS5** the gold complex **3a** is leaving from a coordination position trans to $C_6F_5^-$, which has a high *trans influence*, while in **TS3** it is leaving from a coordination position *trans* to $AsPh_3$, which has a low *trans influence*. The profiles also predict that, although the formation of **1ab** is faster, the concentration at equilibrium should be higher for **2ab** than for **1ab** according to the ΔG^o values of the two profiles. These two predictions of calculations exactly match the experimental results in Figure 3, where the initial higher rate of formation of **1ab** (line of red asterisks) increases quickly its concentration; it then reaches a maximum, and after 1 hour this concentration starts to decrease in favor of **2ab** (line of blue x signs), which after 4.5 h equals and then overpasses the line of **1ab**. All these experimental details support solidly the good approximation to the real system achieved with the calculations.

The two profiles discussed so far require one or two successive AuL migrations to the contiguous aryl, which occur *via* relatively flat geometries (Au is not far from the Pd square plane). In our initial paper,[1] inspired by the two X-ray Pt–Au structures known at that time we had proposed a pyramidal structure from which direct cis or trans exchanges could be achieved almost indistinctly (Scheme 1). This possibility was submitted to calculation and the results (Figure 6, red lines) show that a pyramidal intermediate **IAP**, with gold at the apical position, can exist at about 24.7 kcal×mol^{-1} for Pd (that is at lower free energy distance than **TS1** or **TS5**). **IAP** is accessible from **I1** or **I3** in a barrierless evolution (at least transition states have not been found). Therefore, our original mechanistic proposal for Pd (for tht as ancillary ligand) has activation energy only somewhat higher (2.8 kcal×mol^{-1}) than the "flat" mechanisms calculated here for $AsPh_3$ as ancillary ligand. Whereas the pathway *via* **IAP** is, trusting the calculated energies, unlikely to have a significant contribution for the exact molecules studied here, the "pyramidal" contribution cannot be discarded for related systems (e.g. with other M, Ar, or L components), as discussed later.

The DFT study provides many interesting details on the changes of the gold role when involved in one or another specific exchange step, namely: *i)* the initial or final L-for-ArAuL exchange (either releasing L or releasing ArAuL coordinated to Pd), which occur *via* **TS1**, **TS2**, etc., and lead to the corresponding intermediates **I1**, **I2**, etc.; *ii)* the AuL exchanges between *cis* aryl groups, which involve the "flat" transition states **TS2** and **TS4**; and *iii*) the direct AuL exchanges between *trans* aryl groups, which involve the "pyramidal" structure **IAP**. In order to discuss this, Table 1 summarizes the relevant calculated bond distances along the profiles in Figures 4 and 5. The highlights in Table 1 are meant to remark the common structural features in the table, as follows: 1) the values in parenthesis indicate what are clearly non-interaction M/Ar distances; 2) the red values correspond to typical σ bond M–Ar bond distances; 3) the blue distances, found in intermediates **I1**, **I2**, **I3**, where the aryl on gold is apparently involved in a very asymmetric Au/Pd bridge, which needs to be analyzed in detail; 4) the green values found in **TS2** and **TS4**, correspond to more moderately asymmetric bridging aryls producing the Au/Pd exchange; 5) additionally the Pd-Au distances are shown throughout the reaction coordinate (first column).

Table 1. Au–Pd and C_{ipso}–Pd and C_{ipso}-Au distances (Å) in the calculated structures of Figures 4 and 5. Sum of covalent radii: $r_{Pd}+r_{Au}$ = 2.75 Å; $r_{Pd}+r_{C(sp2)}$ = 2.12 Å; $r_{Au}+r_{C(sp2)}$ = 2.09 Å (usually somewhat shorter for fluorinated aryls).

d (Å)	Au-Pd	Rf¹-Pd	Rf²-Pd	Pf-Pd	Rf¹-Au	Rf²-Au	Pf-Au
TS1	3.35	2.04	2.00	(3.89)	(3.78)	(5.18)	2.05
TS3	3.12	(3.19)	2.06	2.11	2.06	(4.47)	(3.16)
TS5	3.28	2.04	(3.82)	2.00	(3.73)	2.05	(5.08)
I1	2.93	2.03	2.01	*2.63*	(3.70)	(4.80)	2.07
I2	2.95	*2.59*	2.07	2.08	2.07	(3.47)	(3.88)
I3	2.88	2.03	*2.71*	2.00	(3.67)	2.07	(4.78)
TS2	2.88	*2.14*	2.04	*2.18*	*2.32*	(4.53)	*2.38*
TS4	2.91	*2.15*	*2.16*	2.05	*2.29*	*2.45*	(4.49)
IAP	2.70	2.04	2.09	2.10	(3.66)	(3.63)	(3.31)

At first glance, the Au-Pd distances are long (≥ 3.12 Å) in **TS1**, **TS3**, and **TS5**, where the nucleophilic attack by the gold atom is getting involved in an associative L substitution; this interaction will consolidate into shorter Au-Pd distances (2.88-2.95 Å) in the intermediates **I1-I3**, when the L substitution has been completed. Similar or shorter distances (2.88-2.91 Å) are seen in intermediates **TS2** and **TS4**. The shortest Au-Pd distance (2.70 Å, similar to the sum of covalent radii) is found in the pyramidal structure **IAP**.

The initial and final steps of all the calculated pathways resemble a classical associative ligand substitution at square-planar complexes in which the gold complex plays the role of the entering ligand at the beginning of the substitution and that of the leaving ligand at the end of the profile, while $AsPh_3$ plays the other role. In the three corresponding transition states, **TS1**, **TS3**, and **TS5**, the Au and Pd nuclei retain their own initial M–Ar bonds essentially unaltered (see Table 1). For instance, in **TS1** (Figure 6 and Table 2) we find three short M–C(aryl) distances (in the range 2.00-2.05 Å), while the M-C_{ipso} distances to aryls other than their own are very long (3.78-5.18 Å).[43] The long Au···Pd distance already supports an incipient interaction at 3.35 Å (the sum of covalent radii of Pd and Au is 2.75 Å).[44] The As–Au–C_{ipso} angle is 159.6°, suggesting incipient tri-coordination of gold.

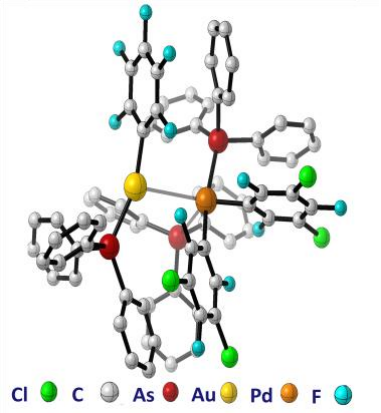

Figure 6. Optimized calculated structure of **TS1**, with hydrogen atoms omitted for clarity**.**

The **I1**-**I3** intermediates can be described as square-planar Pd complexes in which the Au–C_{ipso} bond is occupying one coordination position of the palladium coordination plane, in such a way that their C_{ipso} and Au atoms are, respectively, above and below the Pd coordination plane (Figure 7). The rest of M–Ar or M–As bonds are conventional single bonds and do not need to be discussed. For **I1**, the Pd–Au distance (2.93 Å) is only slightly longer than the expected covalent bond distance; the Au–C_{ipso}(Pf) is also only slightly larger than for terminal Pf groups. Although the Pd–C_{ipso}(Pf) distance is fairy long (2.63 Å), the Au-Pd-Rf angle (152.4°) suggests C_{ipso} π implication in bonding to Pd.[45] In fact the C_{ipso} atom is closer to the calculated square plane of Pd than the Au atom.

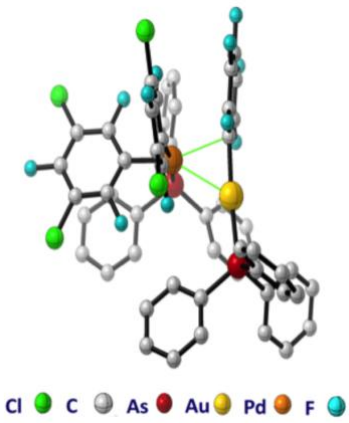

Figure 7. Optimized calculated structure of **I1**. Hydrogen atoms omitted for clarity**.**

In keeping with the previous comments, QTAIM analysis[46] finds bonding critical points between gold and palladium, gold and carbon, and palladium and carbon, consistent with a three-center two-electrons bond. In other words, the Au complex is acting as a ligand side-on coordinated to Pd, through σ-donation from the C_{ipso}–Au bond.

The concerted migration of LAu to the adjacent Rf-Pd bond in intermediate **I2** takes place *via* **TS2** (Figure 8), which displays an almost flat geometry: the four atoms involved in the concerted bond rearrangement are close to coplanar. The Au–Pd distance is in the order of a covalent bond, and the bridging C_{ipso}–M distances to Pd (2.14 and 2.18 Å) are somewhat shorter than to gold (2.32 and 2.38 Å). Also the Pd–C_{ipso} bonds are close to the plane of their corresponding aryls (164.7° and 167.7°), whereas the opposite happens to the Au–C_{ipso} bonds (117.3° and 116.9°), which are much smaller.

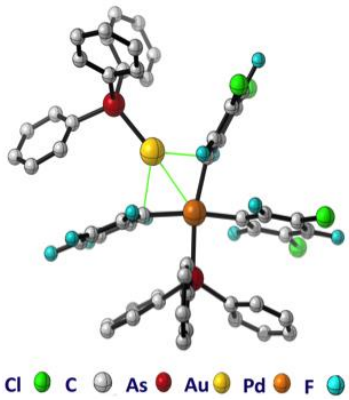

Figure 8. Optimized calculated structure of **TS2** (apical view).

Since the planes of the Rf and Pf groups in **TS2** make an angle much closer to 180° to the terminal C_{ipso}–Pd bonds than the C_{ipso}–Au bonds, the geometry of **TS2** invites to describe the structure as the result of chelating coordination of the two bridging C_{ipso} atoms of the $[\{(Rf)(AsPh_3)\}Pd(Pf)(Rf)]^-$ anion to a $[Au(AsPh_3)]^+$ cation. Of course this model is assuming the net transfer of electron density from the gold moiety to the Pd fragment, which will be partially returned upon coordination of the C_{ipso} atoms to the $(Ph_3As)Au^+$ acidic center. The analysis of **TS2** (and the similar **TS4**) is most interesting In spite of the short distance between the two metals (2.88 and 2.91 Å, respectively), QTAIM analyses does not detect any direct Pd-Au orbital interaction. Consistent with these results, the Mayer bond indexes[47] for Au–Pd are very small (0.0989 for **TS2**). All the orbital interactions are diverted to the bridges, as recently reported for Ru–H–Zn–C systems.[48]

Finally, for the "pyramidal" pathway, the structure of the **IAP** intermediate can be conceived as an anionic $[Pd(Pf)(Rf)_2(AsPh_3)]^-$ fragment making a dative Pd→Au bond to the $[Au(AsPh_3)]^+$ cation (Figure 9). Anionic Pt (and more occasionally Pd) complexes are well known to act as bases towards acidic centers (e.g. Ag^I, Sn^{II}, Pb^{II}, Hg^{II},or Tl^I), forming dative bonds.[49] In fact, QTAIM analysis finds in **IAP** a critical point between Pd^{II} and Au^I (Mayer bond index 0.4222) supporting this proposal. In the evolution for Au to give rise to formation of $PfAu(AsPh_3)$ or $RfAu(AsPh_3)$ after exchange, the

Au atom should receive electron density from the C_{ipso} atoms to make one Au-Ar-Pd single bridge as one of those in **TS2** (Figure 8). Although we have failed to find the putative transition state for this evolution, possibly energetically flat, this exchange must necessarily involve polarization of electron density from Pd to the specific C_{ipso} atom that is getting involved in the exchange, at the expense of the Pd→Au bond.

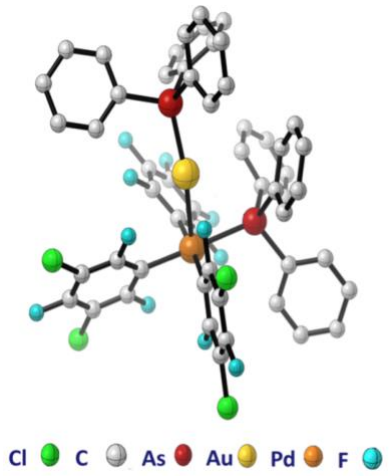

Figure 9. Optimized calculated structure of **IAP**, with hydrogen atoms omitted for clarity.

Note that **TS2** and **TS4** produce exchanges between cis Ar groups, affording a trans exchange only by successive application of two cis exchanges. In contrast, **IAP** can produce cis or trans exchanges directly (except for some small activation energy difference) in just one step.

As mentioned above, the results of the calculations disfavor the **IAP** arrangement for the specific Pd case studied here, although it lays only 3.6 or 2.8 kcal×mol^{-1} higher than **TS2** or **TS4** (Figure 5), respectively. This difference should be easily accessible within the range of energy variations upon change of the metal, the Ar groups being exchanged, the ancillary ligands, or even the solvating solvent. In fact, this kind of trans-to-trans "pole-vaulting" has been proposed recently, with the name "metronome like" mechanism, for the switching of an AuL group between the two C_{ipso} atoms of the aryls in the pincer complex [Pt(CNC)(AuL)(L)](ClO$_4$) (L = PPh$_3$; CNC = 2,6-diphenylpyridinate). Different to our case, in that complex the switching is confined in itself and cannot progress further to release AuArL.[11]

In order to check with a more direct source of information the viability of the catalytic isomerization via **IAP** in other circumstances, the effect of changing Pd for Pt on the molecules of the pathways in Figures 4 and 5 was calculated, taking as zero the energy of **I2** (Figure 10). We were pleased to see that, as hypothesized, this change provokes a switch of the preferred isomerization pathway: Pt prefers the pyramidal transition by 5.9 kcal×mol^{-1}, whereas Pd prefers the flat transition by only 2.8 kcal×mol^{-1}. This supports that the pyramidal preference proposed initially from the Pt the X-ray structures taken as model in 1998, is correct for Pt, and may be misleading for Pd but only by little energy difference. Overall, the study confirms that in other related chemical systems either **TS2**-**TS4** or **IAP** could be preferred.

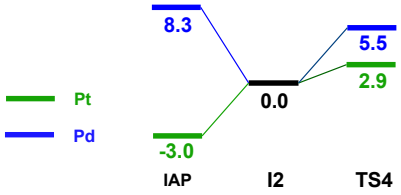

Figure 10. ωB97X-D/def2TZVP(SMD,CHCl$_3$) calculated free energy differences between the transition states **TS4** and **IAP** (Figure 6) for Pd (blue) and Pt (green), taking as zero reference **I2** for each metal.

Conclusions. The *cis/trans* isomerization of diaryl-Pd complexes [Pd(Ar)(Ar')L$_2$] by aryl-gold [AuArL] complexes can occur with or without isomerization. The reactions are initiated by substitution of one ancillary L in Pd for the Au–C_{ipso} bond of the entering [AuArL] molecule, giving eventually an intermediate with asymmetric Pd-Au and Pd-C_{ipso} interaction. From that point, successive aryl exchanges can move the AuL fragment to other aryl in cis, via asymmetric double aryl bridged transition states. The transmetalation barriers are modest (< 12 kcal×mol^{-1} from the corresponding intermediates). Along this "flat" trip, the gold atom remains close to the Pd coordination plane. This is the pathway computationally favored for Ar = Pf, Rf and L = AsPh$_3$.

In a different pathway starting from the same initial intermediates, the gold center transfers its aryl to Pd, and AuL takes the apical position of a square pyramid, remaining connected to Pd by a Pd→Au bond. From its apical position the gold atom can pivot around the Pd→Au bond and directly extract any of the three aryls as [AuAr(AsPh$_3$)], at the expense of the Pd→Au bond, in order to complete the exchange. This pathway coincides with our original proposal,[1] but is about 3 kcal×mol^{-1} higher in energy for the exact Pd case studied. However it cannot be excluded to be preferred for similar systems with different Ar, L, or M. As a matter of fact, with the same groups and ligand used for Pd, the apical pathway is largely preferred for Pt. That this route is the one most favorable when Pd is replaced for Pt in the same complexes, is perhaps to be expected from the participation of the two metals (Au and Pt) with the highest tendency to produce M-M' interactions.

The different features of the Au-Pd interactions along the reaction are a fascinating exhibition of the flexibility of electron density of the metal centers. Au-Pd distances ≥ 3.12 Å, corresponding to weak metallophilic interactions, are found in the transition states for AsPh$_3$ associative substitution **TS1**, **TS3** and **TS5**. The intermediates **I1**, **I2**, and **I3** derived therefrom show much shorter distances (2.88-2.95 Å) corresponding to the formation of Au–C_{ipso}–Pd electron deficient bridges. In **TS2** or **TS4** the formation of asymmetric Au–C_{ipso}–Pd bridges compensating the electron deficiency of the Au(AsPh$_3$)$^+$ fragment is responsible for the geometry and conducts all the orbital interactions through the bridges. In spite of the short Au-Pd distance no QTAIM critical point connecting the two metals is found. Finally, **IAP** displays a clear Pd→Au covalent bond with the shortest bond distance (2.70 Å), possibly due to the existence of several additional bridging interactions with three C_{ipso} and one As atom in the coordination plane of Pd.

The Supporting Information is available free of charge on the ACS Publications website and includes all the experimental and calculation details.

AUTHOR INFORMATION

Corresponding Authors

* P. E.: espinet@qi.uva.es

* R. A.: rar@uvigo.es

* J. A. C.: casares@qi.uva.es

Present address M.H,P-T: Institute of Chemical Research of Catalonia (ICIQ), Avgda. Països Catalans 16, 43007 Tarragona, Spain.

Notes

Dedicated to Kilian Muñiz, who has recently passed away, very prematurely, while working in his office on his life passion, chemistry.

ACKNOWLEDGMENTS

The authors thank the Spanish MINECO (projects CTQ2016-80913-P and CTQ2017-89217-P), the Junta de Castilla y León (projects VA051P17 and VA062G18), and the Xunta de Galicia (Consolidación GRC ED431C2017/61 from DXPCTSUG; ED-431G/02-FEDER "Unha maneira de facer Europa" to CINBIO, a Galician research center 2016−2019), for financial support, as well as CESGA for generous allocation of computational resources.

REFERENCES

1 Casado, A. L.; Espinet, P. A Novel Reversible Aryl Exchange Involving Two Organometallics: Mechanism of the Gold(I)-Catalyzed Isomerization of trans-[PdR_2L_2] Complexes (R = Aryl, L = SC_4H_8) *Organometallics* **1998**, *17*, 3677-3683.

2 (a) Albinati, A.; Lehner, H.; Venanzi, L. M.; Wolfer, M. Silver- and Gold-Containing Heterobinuclear Hydrido-Bridged Complexes. *Inorg. Chem.* **1987**, *26*, 3933–3939. (b) 18) Usón, R.; Forniés, J.; Tomás, M.; Ara, I.; Casas, J. M.; Martín, A. Neutral and Anionic Binuclear Perhalogenophenyl Platinum-Silver Complexes with Pt→Ag Bonds Unsupported by Covalent Bridges. Molecular Structures of [(tht)(C_6F_5)(C_6F_5)$_2$PtAg(PPh_3)], [NBu_4][(C_6F_5)$_4$PtAg(tht)] and [NBu_4][*cis*-(C_6F_5)(C_6F_5)$_2$PtAg(tht)] (tht = tetrahydrothiophene) *J. Chem. Soc., Dalton Trans.* **1991**, 2253-2264.

3 a) Pérez-Temprano, M. H.; Casares, J. A.; Espinet, P. Bimetallic Catalysis using Transition and Group 11 Metals: An Emerging Tool for C–C Coupling and Other Reactions. *Chem. Eur. J.* **2012**, *18*, 1864–1884; b) Pye, D. R.; Mankad, N. P. Bimetallic catalysis for C–C and C–X coupling reactions. *Chem. Sci.* **2017**, *8*, 1705–1718.

4 Crespo, O.; Laguna, A.; Fernández, E. J.; López-de-Luzuriaga, J. M.; Jones, P. G.; Teichert, M.; Monge, M.; Pyykko, P.; Runeberg, N.; Schutz, M.; Werner, H.-J. Experimental and Theoretical Studies of the d^8–d^{10} Interaction between Pd(II) and Au(I): Bis(chloro[(phenylthiomethyl)diphenylphosphine]gold(I))-Dichloro-palladimn(II) and Related Systems. *Inorg. Chem.* **2000**, *39*, 4786–4792.

5 Xia, B.-H.; Zhang, H.-X.; Che, C.-M.; Leung, K.-H.; Phillips, D. L.; Zhu, N.; Zhou, Z.-Y. Metal−Metal Interactions in Heterobimetallic d^8–d^{10} Complexes. Structures and Spectroscopic Investigation of [M'M"(μ-Dcpm)$_2$(CN)$_2$] + (M' = Pt, Pd; M" = Cu, Ag, Au) and Related Complexes by UV−vis Absorption and Resonance Raman Spectroscopy. *J. Am. Chem. Soc.* **2003**, *125*, 10362–10374.

6 Wächtler, E.; Privér, S. H.; Wagler, J.; Heine, T.; Zhechkov, L.; Bennett, M. A.; Bhargava, S. K. Metallophilic Contacts in 2-$C_6F_4PPh_2$ Bridged Heterobinuclear Complexes: A Crystallographic and Computational Study. *Inorg. Chem.* **2015**, *54*, 6947–6957.

7 Gericke, R.; Bennett, M. A.; Privér, S. H.; Bhargava, S. K. Formation of Heterobimetallic Complexes by Addition of d^{10}-Metal Ions to Cis-[(Dppe)M(κ C-2-$C_6F_4PPh_2$)$_2$] (M = Ni, Pd, and Pt). *Organometallics* **2017**, *36*, 3178–3188.

8 Yili, S.; Ramgren, S. D.; Blum, S. A. Palladium-Catalyzed Carboauration of Alkynes and Palladium/Gold Catalyzed Cross-Coupling. *Organometallics* **2009**, *28*, 1275–1277.

9 Reitsamer, C.; Schuh, W.; Kopacka, H.; Wurst, K.; Peringer, P. Synthesis and Structure of the First Heterodinuclear PCP-Pincer-CDP Complex with a Pd-Au d^8-d^{10} Pseudo-Closed-Shell Interaction. *Organometallics* **2009**, *28*, 6617–6620

10 Oeschger, R. J.; Chen, P. Structure and Gas-Phase Thermochemistry of a Pd/Cu Complex: Studies on a Model for Transmetalation Transition States. *J. Am. Chem. Soc.*, **2017**, *139*, 1069–1072.

11 Baya, M.; Belío, Ú.; Fernández, I.; Fuertes, S.; Martín, A. Unusual Metal-Metal Bonding in a Dinuclear Pt-Au Complex: Snapshot of a Transmetalation Process. *Angew. Chem. Int. Ed.* **2016**, *55*, 6978–6982.

12 Pérez-Iglesias, M.; Lozano-Lavilla, O.; Casares, J. A. [Cu($C_6Cl_2F_3$)(tht)]$_4$: An Extremely Efficient Catalyst for the Aryl Scrambling between Palladium Complexes. *Organometallics*, **2019**, *38*, 739-742.

13 del Pozo, J.; Gioria, E.; Casares, J. A.; Álvarez, R.; Espinet P. Organometallic Nucleophiles and Pd: What Makes $ZnMe_2$ Different? Is Au Like Zn? *Organometallics* **2015**, *34*, 3120-3128.

14 Paenurk, E.; Gershoni-Poranne, R.; Chen, P. Trends in Metallophilic Bonding in Pd–Zn and Pd–Cu Complexes. *Organometallics*, **2017**, *36*, 4854–4863.

15 For reviews see: (a) Pérez-Temprano, M. H.; Casares, J. A.; Espinet, P. Bimetallic Catalysis Using Transition and Group 11 Metals: An Emerging Tool for C-C Coupling and Other Reactions. *Chem. - A Eur. J.* **2012**, *18*, 1864–1884. (b) Hirner, J. J.; Shi, Y.; Blum, S. A. Organogold Reactivity with Palladium, Nickel, and Rhodium: Transmetalation, Cross-Coupling, and Dual Catalysis. *Acc. Chem. Res.* **2011**, *44* (8), 603–613.

16 Roth, K. E.; Blum, S. A. Direct Observation of Gold/palladium Transmetalation in an Organogold Heck Reaction. *Organometallics* **2011**, *30*, 4811–4813.

17 Suraru, S. L.; Lee, J. A.; Luscombe, C. K. Preparation of an Aurylated Alkylthiophene Monomer via C-H Activation for Use in Pd-PEPPSI-iPr Catalyzed-Controlled Chain Growth Polymerization. *ACS Macro Lett.* **2016**, *5*, 533–536.

18 Carrasco, D.; Pérez-Temprano, M. H.; Casares, J. A.; Espinet, P. Cross Alkyl-Aryl versus Homo Aryl-Aryl Coupling in Palladium-Catalyzed Coupling of Alkyl-gold(I) and Aryl-Halide. *Organometallics* **2014**, *33*, 3540–3545.

19 Peña-López, M.; Ayán-Varela, M.; Sarandeses, L. A.; Pérez Sestelo, J. Palladium-Catalyzed Cross-Coupling Reactions of organogold(I) Reagents with Organic Electrophiles. *Chem. Eur. J.* **2010**, *16*, 9905–9909.

20 Peña-Lõpez, M.; Sarandeses, L. A.; Pérez Sestelo, J. Organogold(I) Phosphanes in Palladium-Catalyzed Cross-Coupling Reactions in Aqueous Media. *Eur. J. Org. Chem.* **2013**, *13*, 2545–2554.

21 Peña-López, M.; Ayán-Varela, M.; Sarandeses, L. a.; Sestelo, J. P. Palladium-Catalyzed Cross-Coupling Reactions of Organogold(i) Phosphanes with Allylic Electrophiles. *Org. Biomol. Chem.* **2012**, *10*, 1686.

22 Shi, Y.; Peterson, S. M.; Haberaecker, W. W.; Blum, S. a. Alkynes as Stille Reaction Pseudohalides: Gold- and Palladium-

Cocatalyzed Synthesis of Tri- and Tetra-Substituted Olefins. *J. Am. Chem. Soc*. **2008**, *130*, 2168–2169.

23 Shi, Y.; Roth, K. E.; Ramgren, S. D.; Blum, S. A. Catalyzed Catalysis Using Carbophilic Lewis Acidic Gold and Lewis Basic Palladium: Synthesis of Substituted Butenolides and Isocoumarins. *J. Am. Chem. Soc.* **2009**, *131*, 18022–18023.

24 García-Domínguez, P.; Nevado, C. Au-Pd Bimetallic Catalysis: The Importance of Anionic Ligands in Catalyst Speciation. *J. Am. Chem. Soc.* **2016**, *138*, 3266–3269.

25 Hirner, J. J.; Roth, K. E.; Shi, Y.; Blum, S. A. Mechanistic Studies of Azaphilic versus Carbophilic Activation by gold(I) in the Gold/palladium Dual-Catalyzed Rearrangement of Alkenyl Vinyl Aziridines. *Organometallics* **2012**, *31*, 6843–6850.

26 Al-Amin, M.; Johnson, J. S.; Blum, S. A. Selectivity, Compatibility, Downstream Functionalization, and Silver Effect in the Gold and Palladium Dual-Catalytic Synthesis of Lactones. *Organometallics* **2014**, *33*, 5448–5456.

27 delPozo, J.; Casares, J. A.; Espinet, P. The Decisive Role of Ligand Metathesis in Au/Pd Bimetallic Catalysis. *Chem. Commun.* **2013**, *49*, 7246–7248.

28 del Pozo, J.; Carrasco, D.; Pérez-Temprano, M. H.; García-Melchor, M.; Álvarez, R.; Casares, J. A.; Espinet, P. Stille Coupling Involving Bulky Groups Feasible with Gold Cocatalyst. *Angew. Chem. Int. Ed.* **2013**, *52*, 2189–2193.

29 Pérez-Temprano, M. H.; Casares, J. A.; de Lera, Á. R.; Álvarez, R.; Espinet, P. Strong Metallophilic Interactions in the Palladium Arylation by Gold Aryls. *Angew. Chem. Int. Ed.* **2012**, *51*, 4917–4920.

30 Hansmann, M. M.; Pernpointner, M.; Döpp, R.; Hashmi, A. S. K. A Theoretical DFT-Based and Experimental Study of the Transmetalation Step in Au/Pd-Mediated Cross-Coupling Reactions. *Chem. Eur. J.* **2013**, *19*, 15290–15303.

31 Ariafard, A.; Rajabi, N. A.; Jalali Atashgah, M.; Canty, A. J.; Yates, B. F. Computational Study of Carbostannylation Implicating Bimetallic Catalysis involving "Au^{I}-Vinyl-Pd^{II}" species. *ACS Catal.* **2014**, *4*, 860–869.

32 Larsen, M. H.; Nielsen, M. B. The Gilded Edge in Acetylenic Scaffolding II: A Computational Study of the Transmetalation Processes Involved in Palladium-Catalyzed Cross-Couplings of Gold(I) Acetylides. *Organometallics* **2015**, *34*, 3678–3685.

33 Khaledifard, Y.; Nasiri, B.; Javidy, S. A.; Vaziri Sereshk, A.; Yates, B. F.; Ariafard, A. Phosphine-Scavenging Role of Gold(I) Complexes from $Pd(PtBu_3)_2$ in the Bimetallic Catalysis of Carbostannylation of Alkynes. *Organometallics* **2017**, *36*, 2014–2019.

34 Peñas-Defrutos, M. N.; Bartolomé, C.; García-Melchor, M.; Espinet, P. $Rh^{I}Ar/Au^{I}Ar$' Transmetalation: A Case of Group Exchange Pivoting on the Formation of M–M' Bonds through Oxidative Insertion. *Angew. Chem. Int. Ed.*, **2019**, *58*, 3501–3505.

35 For the importance of isomerization in cross-coupling see: Cordovilla, C.; Bartolomé, C.; Martínez-Ilarduya, J. M.; Espinet, P. The Stille Reaction, 38 Years Later. *ACS Catal.* **2015**, *5*, 3040−3053.

36 In previous papers we have shown that both fluoroarilated groups (C_6F_5 and $C_6Cl_2F_3$) are quasi-equivalent and their exchange in identical complexes products almost statistical mixtures at equilibrium. See ref. 37.

37 For some studies using C_6F_5 and $C_6Cl_2F_3$ as labels in mutual exchange reactions see: (a) Casado, A. L.; Casares, J. A.; Espinet P. An Aryl Exchange Reaction with Full Retention of Configuration of the Complexes: Mechanism of the Aryl Exchange between $[PdR_2L_2]$ Complexes in Chloroform (R = pentahalophenyl, L = thioether). *Organometallics*, **1997**, *16*, 5730-5736. (b) Casares, J. A.; Espinet, P.; Soulantica, K.; Pascual I.; Orpen A. G.; $P(CH_2CH_2Py)_nPh_{3-n}$ (Py = 2-Pyridyl; n = 1, 2, 3) as Chelating and as Binucleating Ligands for Palladium. *Inorg. Chem*., **1997**, *36*, 5251-5256. (c) Peñas-Defrutos, M. N.; Bartolomé, C.; García-Melchor, M.; Espinet, P. Hidden aryl-exchange processes in stable 16e Rh^{III} $[RhCp^*Ar_2]$ complexes, and their unexpected transmetalation mechanism. *Chem. Commun.*, **2018**, *54*, 984–987. (d) Peñas-Defrutos, M. N.; Bartolomé, C.; García-Melchor, M.; Espinet, P. Rh IAr/Au IAr' Transmetalation: A Case of Group Exchange Pivoting on the Formation of M–M' Bonds through Oxidative Insertion. *Angew. Chem. Int. Ed.* **2019**, *58*, 3501–3505.

38 The slowness of the uncatalyzed reaction makes some decomposition pathways accessible: thus during the non catalyzed isomerization the starting complex *cis*-$[Pd(C_6Cl_2F_3)_2(AsPh_3)_2]$ reacts also with the solvent, $CDCl_3$, giving *trans*-$[Pd(C_6Cl_2F_3)Cl(AsPh_3)_2]$ (**4**) and $C_6Cl_2F_3D$. However, in the presence of gold catalyst the formation of **4** was kinetically irrelevant in the times used for the kinetic study, and traces of **4** were only observed at much larger times and in the absence of added $AsPh_3$.

39 This experimental value was determined from the integrated signals on the ^{19}F NMR spectrum at equilibrium.

40 The catalytic reaction takes place efficiently with a largely sub-stoichiometric amount of the gold complex **3a**, which in fact acts as catalysts. However, for practical reasons, in order to have a reasonable reaction rate and also to make kinetically irrelevant the non-catalyzed isomerization, concentrations of **3a** close to the stoichiometric value were used in most of the kinetic experiments.

41 □B97XD/def2SVPP_LANL2DZ(SMD,$CHCl_3$)//□B97XD/ def2TZVP(SMD,$CHCl_3$); see details in SI.

42 Complexes **1a**/**3b, 2ab/3a**, and **1ab/3a** were optimized in vitro as unimolecular entities **1a**+**3b, 2ab**+**3a**, and **1ab**+**3a**, on which the exchange processes start. Different conformations were analyzed. The lower energy conformation of the entities **1a**+**3b, 2ab**+**3a**, and **1ab**+**3a** was the one in which the $AsPh_3$ of the gold complex was located near the ligand that dissociates from palladium. The presence of π-stacking interactions between Rf groups of the palladium and Ph groups of $AsPh_3$ in **1a**+**3b, 2ab**+**3a**, and **1ab**+**3a** favors the approximation between the two components, and stabilizes the entity. As it happens often, this association is not experimentally observed in solution, where the overall balance of solvation and entropic effects leads to non-associated molecules.

43 Chemcraft-graphical software for visualization of quantum chemistry computations. https://www.chemcraftprog.com

44 Cordero, B.; Gómez, V.; Platero-Prats, A. E.; Revés, M.; Echeverría, J.; Cremades, E.; Barragán F.; Alvarez, S. Covalent radii revisited. *Dalton Trans*., **2008**, 2832–2838.

45 The space occupied by the aromatic ring of an aryl, spans approximately 1.7 Å above and below the aryl plane. With a covalent r_{Pd} = 1.39 Å, any distance noticeably shorter that 3.09 Å is suggestive of orbital interaction (covalent bonding).

46 (a) Bader, R. F. Atoms in Molecules. *Acc. Chem. Res.* **1985**, *18*, 9–15. (b) Bader, R. F. A Quantum Theory of Molecular Structure and its Applications. *Chem. Rev.* **1991**, *91*, 893–928.

47 (a) Mayer, I. Charge, Bond Order and Valence in the AB initio SCF Theory. *Chem. Phys. Lett.* **1983**, *97*, 270–274; (b) Mayer, I.; Salvador, P. Overlap Populations, Bond Orders and Valences for "Fuzzy" Atoms. *Chem. Phys. Lett.* **2004**, *383*, 368–375.

48 Miloserdov, F. M.; Rajabi, N. A.; Lowe, J. P.; Mahon, M. F.; Macgregor, S. A.; Whittlesey, M. K. Zn-Promoted C–H Reductive Elimination and H_2 Activation via a Dual Unsaturated Heterobimetallic Ru-Zn Intermediate. *J. Am. Chem. Soc.*, Just Accepted Manuscript • DOI: 10.1021/jacs.0c01062 •.

49 There is a nice collection of papers by Forniés and others with structures displaying dative Pt→M, and occasionally Pd→M bonds (M = Ag^{I}, Sn^{II}, Pb^{II}, Tl^{I}). Some representative examples: (a) Usón, R.; Forniés, J.; Tomás, M.; Casas, J. M.; Cotton, F. A.; Falvello, L. R. New Compounds with Platinum to Silver Bonds Unsupported by Covalent Bridges. *J. Am. Chem. Soc.* **1985**, *107*, 2556–2557. (b) Usón, R.; Forniés, J.; Menjón, B.; Cotton, F. A.; Falvello, L. R.; Tomás, M.; Synthesis, X-ray Structure, and Chemical Reactivity of theTetranuclear Cluster $(NBu_4)_2[Pt_2Ag_2Cl_2(C_6F_5)_4]$. X-ray Structure of the Binuclear Compound $(NBu_4)[PtAgCl_2(C_6F_5)_2PPh_3]$. *Inorg. Chem*. **1985**, *24*, 4651–4656. (c) Cotton, F. A.; Falvello, L. R.; Usón, R.; Forniés, J.; Tomás, M.; Casas, J. M.; Ara, I. Heterobinuclear PtAg Compounds with Platinum-Silver Bonds Unsupported by Covalent

Bridges. Molecular Structure of $(C_6F_5)_3(SC_4H_8)PtAgPPh_3$. *Inorg. Chem.* **1987**, *26*, 1366–1370. (d) Usón, R.; Forniés, J. Synthesis and structures of novel types of heteronuclear Pt-M neutral or anionic organometallic complexes. *Inorg. Chim. Acta* **1992**, *198*, 165–177, and references therein. (e) Forniés, J.; Giménez, N.; Ibáñez, S.; Lalinde, E.; Martín, A.; Moreno, M. T. An Extended Chain and Trinuclear Complexes Based on Pt(II)−M (M = Tl(I), Pb(II)) Bonds: Contrasting Photophysical Behavior. *Inorg. Chem.* **2015**, *54*, 4351–4363.